ISSN 0016-7932, Geomagnetism and Aeronomy, 2018, Vol. 58, No. 3, pp. 295–306. © Pleiades Publishing, Ltd., 2018.
Original Russian Text © V.G. Vorobjev, O.I. Yagodkina, E.E. Antonova, V.L. Zverev, 2018, published in Geomagnetizm i Aeronomiya, 2018, Vol. 58, No. 3.

Influence of Solar Wind Plasma Parameters on the Intensity of Isolated Magnetospheric Substorms

V. G. Vorobjev[a], *, O. I. Yagodkina[a], E. E. Antonova[b], and V. L. Zverev[a]

[a] *Polar Geophysical Institute, Apatity Division, Apatity, Murmansk region, 184209 Russia*

[b] *Skobeltsyn Research Institute of Nuclear Physics, Moscow State University, Moscow, 119991 Russia*

**e-mail: vorobjev@pgia.ru*

Received June 27, 2017

Abstract—Parameters of the interplanetary magnetic field and solar wind plasma during periods of 163 isolated substorms have been studied. It is shown that the solar wind velocity V and plasma density N remain approximately constant for at least 3 h before substorm onset T_o and 1 h after T_o. On average, the velocity of the solar wind exhibits a stable trend toward anticorrelation with its density over the whole data array. However, the situation is different if the values of V and N are considered with respect to the intensity of substorms observed during that period. With the growth of substorm intensity, quantified as the maximum absolute value of AL index, an increase in both the solar wind plasma velocity and density, at which these substorms appear, is obsreved. It has been found that the magnitude of the solar wind dynamic pressure P is closely related to the magnetosphere energy load defined as averaged values of the Kan–Lee electric field E_{KL} and Newell parameter $d\Phi/dt$ averaged for 1 h interval before T_o. The growth of the dynamic pressure is accompanied by an increase in the load energy necessary for substorm generation. This interrelation between P and values of E_{KL} and $d\Phi/dt$ is absent in other, arbitrarily chosen periods. It is believed that the processes accompanying increasing dynamic pressure of the solar wind result in the formation of magnetosphere conditions that increasingly impede substorm generation. Thus, the larger is P, the more solar wind energy must enter the Earth's magnetosphere during the period of the growth phase for substorm generation. This energy is later released during the period of the substorm expansion phase and creates even more intense magnetic bays.

DOI: 10.1134/S0016793218030155

1. INTRODUCTION

The conception of the classical substorm suggests that solar wind energy is accumulated in the Earth's magnetosphere and then suddenly released during a substorm period, the onset of the expansion phase of which is denoted hereinafter as T_o. The onset of the expansion phase is preceded by the growth phase (McPherron, 1970), the appearance of which is usually associated with a southward turn of the Bz component of the interplanetary magnetic field (IMF). The duration of the substorm growth phase is estimated by different studies to be researcher as 0.5–2 h. According to results of statistical investigation of isolated substorms with a maximum of $|AL| > 300$ nT, the presence of a considerable interval of the southward IMF before T_o was noted (Vorobjev et al., 2016). The average duration of that interval amounted to ~80 min.

The substorm growth phase can be treated as a time interval in which the Earth's magnetosphere is loaded by the solar wind energy. The hypothesis on the presence of the loading phase before the substorm onset has been corroborated by many theoretical and experimental studies (e.g., Russell and McPherron, 1973a; Shukhtina et al., 2005; Boakes et al., 2009). During the period of substorm growth phase, the magnetic pressure in the lobes of the magnetosphere tail increases, geomagnetic field lines extend in the antisolar direction, and the plasma sheet thickness decreases (e.g., Shukhtina et al., 2014). In the long run, these changes lead to the development of some instability in the Earth's magnetosphere. The instability is accompanied by rapid unloading of the accumulated magnetic flux, i.e., by the substorm onset.

Despite numerous investigations carried out in recent decades, many important problems in physics of magnetospheric substorms remain unsolved. This is related to the fact that results of studies carried out by different authors are not always unambiguous and often contradict each other. We dwell only on some of such problems related to the substorm growth phase and loading–unloading processes in the magnetosphere. So, from the analysis of substorms registered by the IMAGE magnetometer network, Kallio et al. (2000) concluded that the energy loading of the magnetosphere during the period of substorm growth phase is necessary exclusively to change its configuration before T_o, while the intensity of the substorm is determined by the flow of energy straightly in the period of the substorm expansion phase. It follows that

the intensity of the subsequent substorm will be very low if the energy inflow to the magnetosphere stops immediately before T_o. This conclusion contradicts earlier results (Lyons, 1996; Lyons et al., 1997) in which the authors suppose that most, or probably all, substorms are triggered by a sharp decrease in the large-scale electric field transferred into the magnetosphere from the solar wind if it is preceded by a growth phase with a duration of >30 min. Moreover, Hsu and McPherron (2004) concluded that substorms triggered by a northward IMF turn are systematically stronger than nontriggered ones. However, according to statistical studies of isolated substorms (Vorobjev et al., 2016), both the duration of the growth phase and the intensity of the magnetic disturbance for substorms occurring at negative and positive IMF polarity are, on average, approximately equal.

Shukhtina et al. (2005) and Milan et al. (2009) showed that the substorm intensity is determined by the total magnetic flux transferred from the daytime magnetosphere to the tail before the onset. However, Li et al. (2013) later concluded that the substorm intensity correlates well with the reconnection electric field magnitude determined by the Kan–Lee formula (Kan and Lee, 1979) but does not depend on the total amount of energy entering the magnetosphere during the period of the growth phase. The conclusion made by Li et al. (2013) may result from two facts—first, the insufficiently correct method of determining the substorm intensity. Li et al. (2013) determined the substorm intensity as the maximum intensity of auroral precipitations measured by the NOAA/POES satellite in an interval of 1.5 h after the substorm expansive phase onset. Since satellite flights through the auroral zone are discrete (approximately 14 orbits during the day), the auroral precipitation power determined in the 1.5 h interval will hardly correspond to its maximum values. Second, the events investigated by Li et al. (2013) are not simple elementary magnetospheric disturbances; instead, they form a series of consecutive substorms. In this situation, it is difficult to find an adequate relation between the energy coming into the magnetosphere during the period of the growth phase and the energy released in a given disturbance interval.

In contrast to conclusions of Li et al. (2013), the close connection between integral values of the energy coming to the magnetosphere during the period of substorm growth phase and total energy of auroral precipitations was shown by Vorobjev et al. (2016). They statistically studied processes of magnetosphere loading–unloading in periods of isolated magnetospheric substorms. The energy connection between the solar wind and magnetosphere was estimated (Vorobjev et al., 2016) with different parameters, in particular, the electric field E_{K-L} (Kan and Lee, 1979) and parameter $d\Phi/dt$ (Newell et al., 2007). The coefficients of correlation between the total energy of auroral precipitations during the period of the substorm and integral values of the functions E_{KL} and $d\Phi/dt$ obtained by Vorobjev et al. (2016) were equal to 0.71 and 0.84, respectively. This is significantly higher than the values of 0.64 and 0.55 obtained (Li et al., 2013) for average hourly values of the functions E_{K-L} and $d\Phi/dt$, respectively.

The substorm intensity varies over a wide range. The magnitude of the *AL* index can amount from several hundreds to several thousands nT. The fundamental question of which factor is control the intensity of substorms, remains still open. There is no doubt that the solar wind plasma and interplanetary magnetic field are the source of the magnetospheric substorm energy. Traditionally, the IMF *Bz* component is believed to be the most efficient for substorm generation. The velocity (V, km/s) and plasma density (N, cm^{-3}) of the solar wind slightly vary on substorm time scales; for this reason, these parameters are usually not considered as autonomous energy sources for substorm disturbances. However, some studies investigations indirectly show the importance of the solar wind kinetic energy in the processes of substorm formation. For example, Barkhatov et al. (2017) outlined the results of experiments on the recovery of variations in the *AL* magnetic activity index during periods of isolated substorms with the use of artificial neural networks. It turned out that the recovery was carried out most efficiently if the role of input sequences is played not only by IMF components but also by the integral parameter $\Sigma[NV^2]$, which takes into account the prehistory of the solar wind kinetic energy pumping into the magnetosphere.

The investigation of substorm activity was studied on large time intervals—diurnal, seasonal, and annual variations (Newell et al., 2013; Newell et al., 2016). It was shown that the probability of substorm appearance is best predicted only by the solar wind velocity, not by more complicated functions including also IMF components. According to those studies, the probability of the appearance of substorms or substorm series significantly increases with an increase in V while the effect of the solar wind dynamic pressure P is insignificant.

In this work, it is hypothesized that quantitative characteristics of the solar wind plasma before the substorm growth phase can lead in the Earth's magnetosphere to the formation of an equilibrium state that will determine to a considerable extent the intensity of the magnetospheric disturbance generated at a later stage. In this work, with that in mind, the behavior of IMF components and solar wind velocity V and plasma density N in periods of the registration of isolated substorms with different intensities is studied, and the interrelation of the quantities V and N with the level of the *AL* index in the substorm maximum is determined. One of main problems of this work is to study the manner in which the parameters of the solar wind plasma affect processes of energy loading of the magnetosphere before the onset of the substorm growth phase. In addition, in the course of the study,

the diurnal distribution of the onset (T_o) is determined for substorms with different intensities and the effect of the *By* IMF component on processes of the formation of the substorm activity is studied.

2. DATA USED

In this work, the studies were carried out with a list of isolated substorms composed earlier (Vorobjev et al., 2016). To extract isolated substorms, we used the diurnal variations (http://wdc.kugi.kyoto-u.ac.jp/) and 1-min digital values (http://cdaweb.gsfc.nasa.gov/) of the *AL* magnetic activity index for all winter seasons of 1995–2013. The isolated substorms were selected with the following criteria:

(1) The temporal interval from the preceding disturbance is not less than 3 h.

(2) The intensity of a magnetic bay is $300 < \mathrm{Max}|AL| < 1300$ nT in maximal.

(3) The substorm duration is <3 h.

(4) The end of substorm is UT after which the disturbance is $|AL| < 0.2\ \mathrm{Max}|AL|$.

The substorms were selected based on criteria 1–3 by visual examination of diurnal variations in the *AL* index, and the time of substorm onset was determined an automatic algorithm. The substorm onset T_o was determined by the time when the difference between two subsequent values of the *AL* index exceeded 60 nT and the next *AL* value differed from the first one as much as by –100 nT. This algorithm was presented in more detail by Vorobjev et al. (2016).

For purposes of this work, the list was supplemented with weak isolated substorms registered in the same time interval with an intensity of $|AL_{\max}| < 300$ nT in the maximum. The onset of such substorms was determined with a simpler criterion $|(AL_n - AL_{n-1})| > 30$ nT, where n is the current 1-min value of the *AL* index.

The parameters of the IMF and solar wind plasma were taken from the OMNIWeb database (http://cdaweb.gsfc.nasa.gov/). For each substorm, these data were taken in an 8-h UT interval with T_o approximately in the middle part of the interval. Only those events for which OMNI data contained no gaps of longer than 10 min were included in the list of isolated substorms. Thus, the total list included 163 substorms with different intensities. The list of isolated substorms can be found at http://pgia.ru/lang/en/data.

3. COMPARATIVE CHARACTERISTICS OF SUBSTORMS WITH DIFFERENT INTENSITIES

The average characteristics of the interplanetary medium and variations in the magnetic activity in the period of registering substorms with an intensity $|AL_{\max}| < 300$ nT and $|AL_{\max}| > 600$ nT in the maximum are shown in Figs. 1a and 1b, respectively. The curves presented in Fig. 1 were obtained by the superposed epoch method in an interval of ±3 h with respect to the T_o. In total, 65 and 44 events of low and high intensity, respectively, have been considered.

It is conspicuous that the values of all parameters considered in Fig. 1 for high-intensity substorms are noticeably higher than their values for small substorms. Namely, small substorms appear at a level of $SYM/H \sim -6$ nT; large ones, at $SYM/H \sim -18$ nT. At small substorms, the average solar wind velocity does not exceed 400 km/s; for large ones, it is greater than 450 km/s. The average solar wind plasma density to ~6 and ~10 cm^{-3} for small and large substorms, respectively. As should be expected, the values of the southward IMF component are considerably larger for substorms with higher intensity. As for the azimuthal IMF component, one can note that low-intensity substorms appear mainly on the background of negative values of the *By* IMF component, while the sign of the *By* component is probably of no particular importance for the generation of large substorms.

The data considered in Fig. 1 are presented in graphical form in Fig. 2. The two groups of high- and low-intensity substorms are supplemented by the third group of substorms, with an intensity of $300 < |AL_{\max}| < 600$ nT in maximum. Figure 2 shows data averaged over 1 (curve *1*), 2 (curve *2*), and 3 h (curve *3*) before the onset T_o. Over the horizontal axis, the plot is represented only by three points corresponding to average values of weak, middle, and high intensity.

The left column (Fig. 2a) shows the solar wind velocity *V* and plasma density *N*. Curves *1*, *2*, and *3* in these figures almost coincide, which is essentially evidence that *V* and *N* vary very slightly, at least in the 3-h interval before the substorm onset. Special attention should be paid to the fact that substorms with a higher intensity appear at the level of ever more increasing values both of *V* and of *N*.

Figure 2b shows the average values of the *SYM/H* and *PC* indices for substorms with different intensities. The values of these indices averaged 1, 2, and 3 h before T_o almost coincide; in addition, let us note that the absolute value of the indices subsequently grows with an increase in the intensity of the following substorm activity.

Figure 2c presents average values of the *Bz* and *By* IMF components. The strongest effect on the intensity of substorms is evidently exerted by the level of the *Bz* IMF component averaged 1 h before the substorm onset (curve *1*). The intervals of 2 and 3 h before the substorm onset (curves *2* and *3*) include both the growth phase and the quiet geomagnetic field period preceding to it. For this reason, values of the southward IMF component on the curves *1*, *2*, and *3* sequentially decrease. The increase in the level of negative *Bz* for substorms with higher intensity also looks natural.

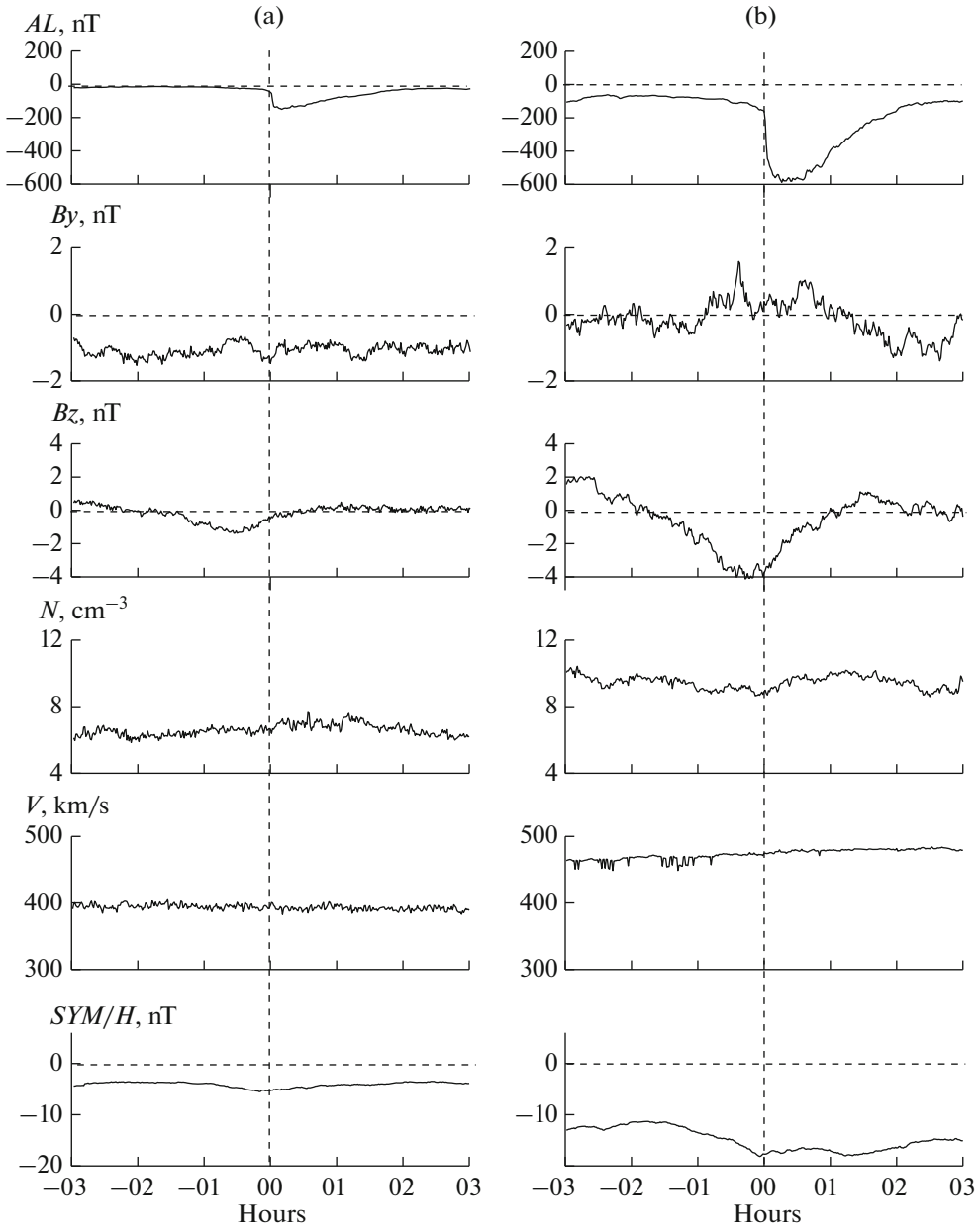

Fig. 1. Average characteristics of the interplanetary medium and magnetic activity for substorms with (a) $|AL_{max}| < 300$ nT and (b) $|AL_{max}| > 600$ nT. The curves were obtained by the superposed epoch method in an interval of ±3 h with respect to T_o. From top to bottom: variations in the *AL* index, *By* and *Bz* IMF components, density *N* and velocity *V* of the solar wind, and values of the *SYM/H* index.

The behavior of the *By* IMF component shown in the lower part of Fig. 2c corroborates the conclusions made earlier from the analysis of Fig. 1. Substorms with low and middle intensity are as a rule preceded by negative values of the *By* IMF component while middle values of *By* for large substorms are zero or weakly positive. These data show that negative values both of *Bz* and *By* IMF components are the most favorable conditions for the generation of low- and middle-intensity substorms. The generation of large substorms needs large negative the *Bz* IMF component; however, the sign of the *By* component is likely to be of no particular importance.

In our opinion, the data shown in Fig. 2a are of the greatest interest. The results show that high-intensity substorms are registered on the background of ever increasing values both of velocity and density of the solar wind. It is well known that the magnitude of the solar wind velocity has a decreasing trend with an increase in the solar plasma density. In particular, high-velocity solar wind fluxes from coronal holes have a low density; at the same time, dense solar wind

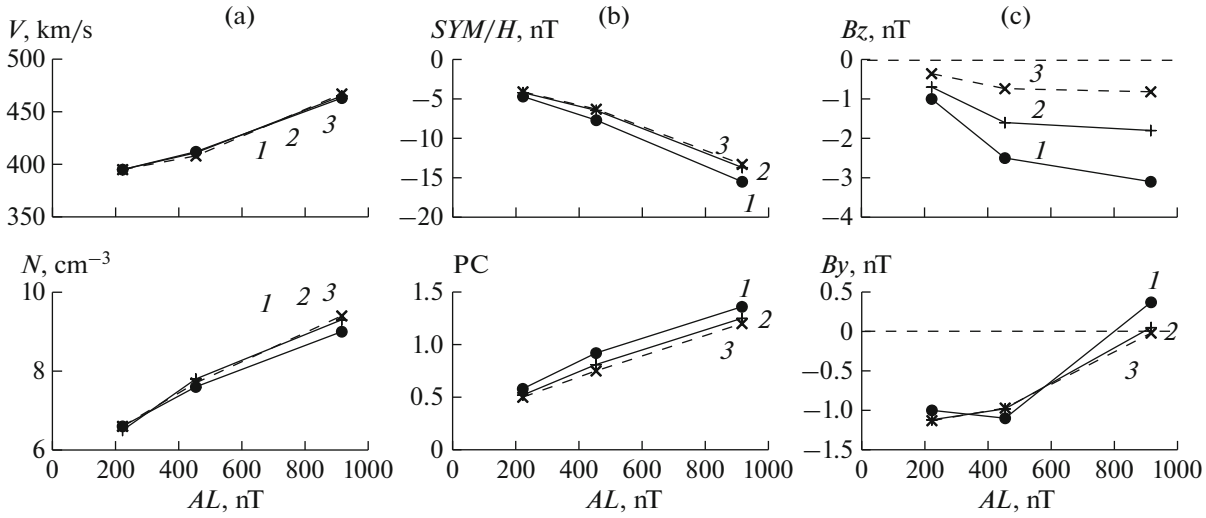

Fig. 2. Average values of the interplanetary medium parameters and magnetic activity indices for a substorm with a low ($|AL_{max}| < 300$ nT, middle ($300 < |AL_{max}| < 600$ nT), and high ($|AL_{max}| > 600$ nT) intensity. The data were averaged over (*1*) 1, (*2*) 2, and (*3*) 3 h before T_o.

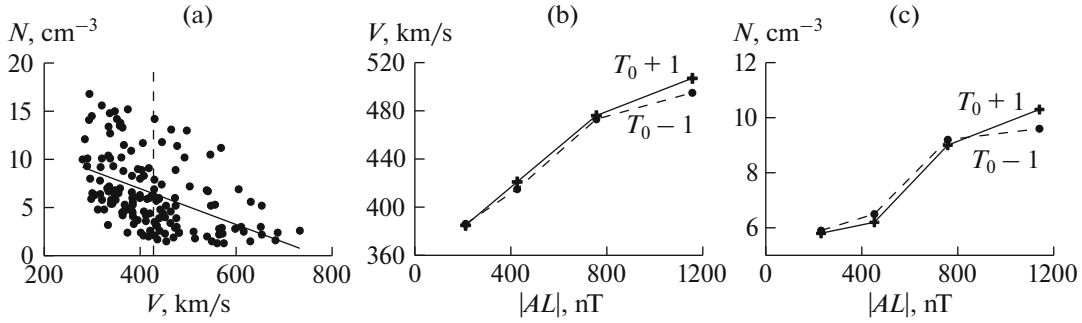

Fig. 3. (a) Relation between the plasma density and velocity of the solar wind. Average values of the (b) velocity and (c) density of the solar wind for substorms with different intensity. All substorms are divided into four groups: $|AL_{max}| < 300$ nT, $300 < |AL_{max}| < 600$ nT, $600 < |AL_{max}| < 900$ nT, and $|AL_{max}| > 900$ nT. Dashed lines show V and N are averaged over 1 h before the onset of the substorm ($T_o - 1$); solid lines show V and N averaged over 1 h after the onset of the substorm ($T_o + 1$).

fluxes in the region of the heliospheric current sheet have relatively low velocities. In our events, this trend is illustrated by Fig. 3a. The figure shows the relation between the plasma density and velocity of the solar wind for all events studied in this work. Figure 3a uses average values of V and N observed 1 h before the T_o. The vertical dashed line shows the average value of the solar wind velocity over the whole data array, ~420 km/s. The solid line corresponds to the linear regression equation. A trend toward a decrease in the plasma density with an increase in the solar wind velocity is discernible rather clearly.

However, the situation is different if values of V and N are considered with respect to the intensity of substorms observed in this period. With an increase in the AL magnetic activity index, an increase is observed in the substorm maximum in the levels both of the velocity and the plasma density of the solar wind, on the background of which substorms appear. This result, which was presented above in Fig. 2a, is additionally illustrated in Figs. 3b and 3c. The substorms in Figs. 3b and 3c are combined into 300 nT groups. The dashed lines in the figures correspond to the V and N data averaged over 1 h before T_o; the solid lines correspond to the data averaged over 1 h after T_o. The solid and dashed lines in Fig. 3b and 3c are very close to each other. This shows that the velocity and density of the solar wind vary insignificantly during the period of the substorm expansion as compared to their level in the period of the substorm growth. The curves in Figs. 3b and 3c demonstrate a steady growth of V and N with an increase in the intensity of substorms observed in that period. So, substorms with intensities $|AL_{max}| < 300$ nT were observed at $V \sim 380$ km/s and $N \sim 5.8$ cm^{-3}; substorms with $|AL_{max}| > 900$ nT were observed at $V \sim 500$ km/s and $N \sim 10.0$ cm^{-3}.

4. MONITORING OF SUBSTORM INTENSITY BY VELOCITY AND DENSITY OF THE SOLAR WIND PLASMA

Special attention should be paid to the following key results of the previous section. The velocity V and plasma density N of the solar wind remain approximately constant for a long time interval, for at least 3 h before the onset T_o and 1 h after T_o. An increase of the intensity of magnetospheric substorms generated in those periods was observed with an increased V and N levels. The results allow one to make a supposition that the quantitative characteristics of solar wind plasma before the onset of the substorm create an equilibrium state in the Earth's magnetosphere that determines to a considerable extent the intensity of the magnetospheric disturbance generated at a later stage. Moreover, we suppose that the increasing V and N values lead to the formation of conditions in the Earth's magnetosphere that increasingly impede substorm generation. Therefore, the higher is the velocity and/or plasma density of the solar wind, the more solar wind energy must be loaded into the Earth's magnetosphere during the period of growth phase for substorm generation. At a later stage, this energy will be released during the substorm expansion phase and create even more intense magnetic bays.

At the first stage, we assume that the Bz IMF component is most effective for substorm generation. Then, if the aforementioned suppositions are valid, a definite relation between Bz and parameters of the solar wind plasma must be implemented in the period of the substorm growth phase. The upper part of Fig. 4 shows the (a) plasma density, (b) velocity, and (c) dynamic pressure of the solar wind relative to the magnitude and sign of the Bz IMF component. The number of dots in the plots corresponds to the total number of studied substorms. Figure 4 uses data averaged over 1 h before the onset of each isolated substorm. The spread of dots is considerable, but the trend toward an increase in the negative Bz IMF component with increasing plasma density and dynamic pressure of the solar wind is clearly discernible.

For better clarity, the lower part of the figure presents the same data but averaged over each interval of Bz by 2 nT. It is seen from the figure that the solar wind velocity remains approximately at its average level, regardless of the Bz sign. However, with an increase of the density N and dynamic pressure P of the solar wind, the values of the southward IMF component registered before the onset of the substorm expansion phase increase. Numerical values of N and P are closely related in the sense that the dynamic pressure is determined mainly by the solar wind plasma density.

The importance of the solar wind velocity value apparently lies in its energy contribution in the period of the growth phase as one of components of the reconnection electric field. It was shown (Vorobjev et al., 2016) that the intensity of isolated substorms correlates best not with the southward IMF component but with the electric field $E_{KL} = VB_T\sin^2(\theta/2)$ (Kan and Lee, 1979), where $B_T = (By^2 + Bz^2)^{1/2}$ and the IMF hour angle $\theta = \arctan(By/Bz)$, or with the parameter $d\Phi/dt = V^{4/3}B_T^{2/3}\sin^{8/3}(\theta/2)$ (Newell et al., 2007). In these expressions, together with the IMF orientation in the YZ plane, a significant part is played by the solar wind velocity, which determines the value of the geomagnetically active interplanetary electric field.

The interrelation between a loading of the magnitosphere by the solar wind energy before the onset and dynamic pressure of the solar wind is demonstrated by Fig. 5. This figure, as Fig. 4, uses data averaged over 1 h before the onset of each substorm. On the horizontal axis, the dynamic pressure (P) is plotted. The dots in the plots show average values of E_{KL} (Fig. 5a) and $d\Phi/dt$ (Fig. 5b) in each interval of P by 2 nPa. The solid lines correspond to the linear regression equations. The segments of the vertical lines show the value of the root-mean-square deviation.

Figure 5 shows the rather close relation between the dynamic pressure and loading of the magnitosphere by the solar wind energy. An increase of the dynamic pressure leads to an increase in the loading energy necessary for substorm generation. The coefficients of correlation over all points of the array (163 substorms) are $r = 0.91$ and 0.85 for the functions E_{KL} and $d\Phi/dt$, respectively.

There are no reason to believe that such a close relation between the dynamic pressure and functions E_{KL} and $d\Phi/dt$ can exist in other arbitrarily chosen periods. For comparison, two intervals were taken: December 10–19, 2000 and December 10–19, 2007. The interval duration was chosen such that the array of hourly data per interval was compared with the array of studied substorms. December corresponds to the middle of the winter period, and 2000 and 2007 correspond to the years of minimum and maximum of solar activity. For these data arrays, the following coefficients of correlation were obtained: in 2000, $r = 0.23$ and 0.21; in 2007, $r = 0.49$ and 0.36 for the functions E_{KL} and $d\Phi/dt$, respectively. The low level of correlation coefficients indicates the absence of relations between P and functions E_{KL} and $d\Phi/dt$. Only in periods preceding to T_o the dynamic pressure will determine the energy of loading which is needed for generation of the substorm.

The results show a good correlation between the dynamic pressure and value of the magnetosphere loading by the solar wind energy before the substorm onset. At the same time, the spread of data presented in Fig. 5 is less than in Fig. 4 but nevertheless remains considerable. On the one hand, this may result from the fact that our studies involved hourly averaged values of interplanetary medium parameters, not integration over the interval of the substorm growth phase.

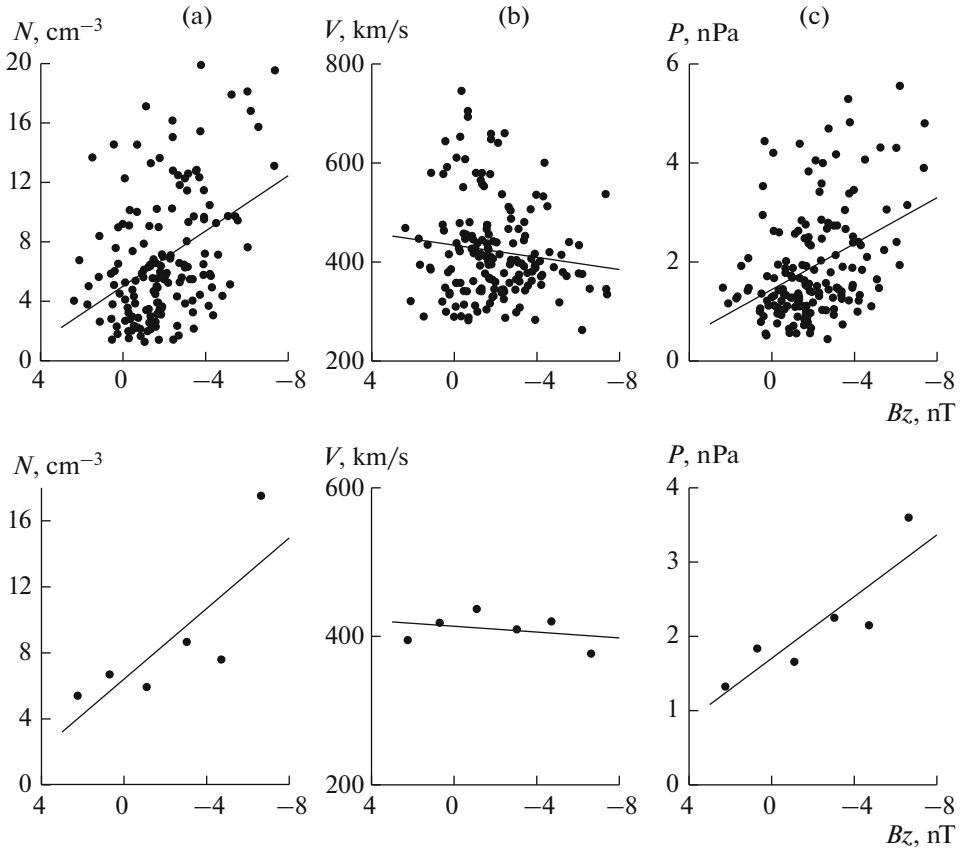

Fig. 4. (a) Plasma density, (b) velocity, and (c) dynamic pressure of the solar wind as functions of the IMF Bz component. The data were obtained by averaging over 1 h before each isolated substorm. The upper panel of the figure shows data over the whole array of the substorms. The lower panel shows the same data but after averaging over intervals of Bz by 2 nT.

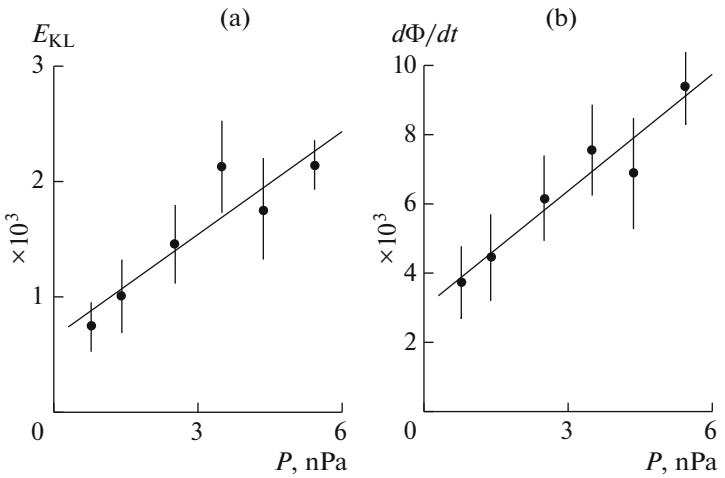

Fig. 5. Value of loading of the magnetosphere by the solar wind energy before the onset of the substorm expansion phase (E_{KL} and $d\Phi/dt$) as functions of the dynamic pressure. The dots in the plots are average values of the functions in each interval of P by 2 nPa. The solid lines are the linear regression equations. The vertical segments are values of the root-mean-square deviation.

On the other hand, the Russell–McPherron effect (Russell and McPherron, 1973b), which is related to the diurnal rotation of the geomagnetic dipole axis, can make a definite contribution to the data spread. Indeed, Fig. 6 shows the histogram of the diurnal distribution of the substorm onset. The vertical axis shows the number of substorms with onset in the corresponding 2-h UT interval. In the intensity, as in Fig. 2, the substorms are divided into (a) weak, (b) moderate, and (c) strong ones.

Figure 6 shows that a maximum of the substorm onset is observed in the interval of 1000–1200 UT of

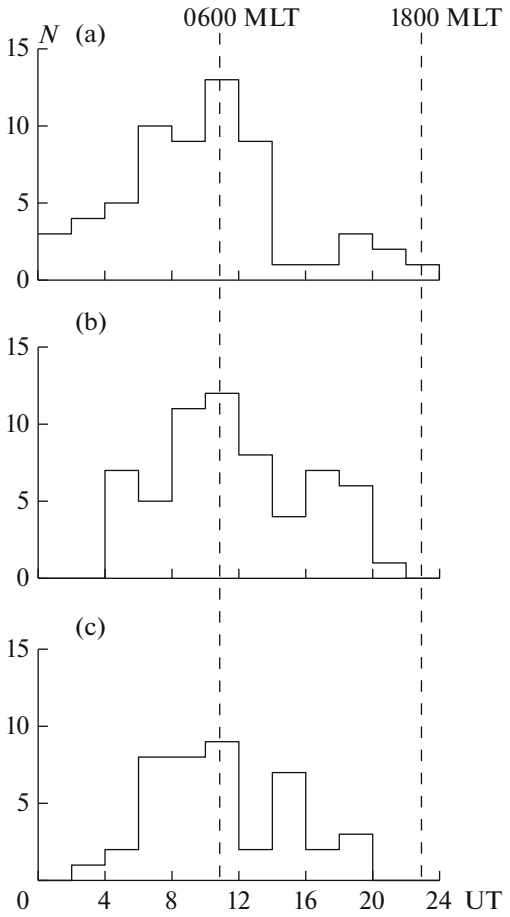

Fig. 6. Diurnal distribution of the onset for substorms with (a) low ($|AL_{max}| < 300$ nT), (b) middle ($300 < |AL_{max}| < 600$ nT), and (c) high ($|AL_{max}| > 600$ nT) intensities. The vertical dashed lines show UT when the geomagnetic dipole axis is tilted toward the morning and evening side.

the diurnal distribution. This maximum is most pronounced for weak substorms (Fig. 6a). For moderate substorms, it expands to the interval of 0800–1200 UT (Fig. 6b); for strong substorms, it looks least clearly and even in a wider interval of 0600–1200 UT. The presence of such a maximum could be treated as a disadvantage of the traditional *AL* index determined by a small number (10–12) of ground-based magnetic stations. However, the presence of the before-midday (UT) maximum in the diurnal distribution of the probability of substorm appearance in winter can be also found in Newell et al. (2013, Fig. 7) investigations. The authors of that work determined T_o by use of the *SML* (SuperMAG Low) index, which is similar to the *AL* index but is determined by data of 130 stations.

The vertical dashed lines in Fig. 6 show UT at which the geomagnetic dipole axis in the GSM coordinate system is tilted along the *Y* axis towards 0600 and 1800 MLT. It is seen in Fig. 6 that the maximum number of low- and middle-intensity substorms are observed in periods when the geomagnetic dipole axis is tilted towards the morning. Such tilt of the dipole axis in combination with negative values of the *By* IMF component, as illustrated by Figs. 1a and 2c, yields the effective negative *Bz* component. Being dependent both on the *By* IMF component and on UT, the magnitude of this component will make a certain contribution to the degree of solar wind geoefficiency before the substorm onset.

5. DISCUSSION

In this work, the parameters of the IMF and solar wind plasma have been studied in the periods of 163 isolated magnetospheric substorms, the list of which can be found on the website http://pgia.ru/lang/en/data. The isolatedness of substorms was determined by the criteria described in Section 2. Isolated substorms were selected based on diurnal variations http://wdc.kugi.kyoto-u.ac.jp/ and 1-min digital values http://cdaweb.gsfc.nasa.gov/ of the *AL* magnetic activity index for all winter seasons from 1995 to 2013. Parameters of the IMF and solar wind plasma were taken from the OMNIWeb database http://cdaweb.gsfc.nasa.gov/.

In the considered events, the solar wind plasma density varied within the limits from ~1 to ~20 cm^{-3}; the velocity, from ~280 to ~700 km/s. The average value of *V* over the whole array was ~420 km/s. As seen in Fig. 3a, the velocity of the solar wind exceeded this average level in a considerable number of the events. Therefore, the thesis (Newell et al., 2016) that isolated substorms appear at low values of the solar wind velocity, not higher than average *V*, lacks support within our data array.

The main results obtained in the scope of the performed investigations can be stated as follows.

1. The velocity (*V*) and plasma density (*N*) of the solar wind remain approximately constant for at least three hours before the onset of the isolated substorm (T_o) and one hour after T_o.

2. On average over the whole data array, the solar wind velocity shows a steady trend toward anticorrelation with the solar wind density. However, the situation is different if *V* and *N* are considered with respect to the substorm intensity observed in this period. With an increase in the $|AL|$ index, an increase is observed in the levels both of the velocity and plasma density of the solar wind on the background of which these substorms appear.

3. The value of the dynamic pressure of the solar wind (*P*) has a significant effect on the energy loading of the magnetosphere defined as average values of the functions E_{KL} and $d\Phi/dt$ which were found during 1 h before the onset of the expansion phase of each substorm. The increase in the dynamic pressure is accompanied by an increase in the loading energy necessary for the generation of substorms. This interconnection between *P* and

values of E_{KL} and $d\Phi/dt$ is absent in other arbitrarily chosen periods.

4. Negative values of the *By* IMF component are the most favorable conditions for the generation of low- and middle-intensity substorms. The sign of the *By* component seems to be of no particular importance in the generation of large substorms with $|AL_{max}| > 600$ nT.

5. In the diurnal distribution of the substorm onset, a maximum was observed in the interval of 1000–1200 UT. In this period, the geomagnetic dipole axis is tilted to the morning side. Such a tilt of the dipole axis in combination with negative values of the *By* IMF component yield an effective negative *Bz* component. The magnitude of this component, which depends both on the *By* IMF and on UT, will make an additional contribution to the degree of solar wind geoefficiency before the substorm onset.

There can be no doubt that main processes in the substorm expansion period occur in the magnetosphere–ionosphere system. The cause of the substorm onset can be classified as one of most frequently discussed questions in the present-day scientific literature. In this work, we do not concern the specificity of instabilities leading to substorm generation but consider some problems that seem to be the most important for the purposes of this study.

The question of whether the substorm generation needs sharp changes in the parameters of the external medium (triggers) or substorms are generated under certain conditions due to the development of an instability inside the magnetosphere remains debatable to date. In particular, Lyons (1996) supposed that most, or probably all, substorms are triggered by a decrease in the large-scale electric field transferred into the magnetosphere from the solar wind if it is preceded by a growth phase with a duration of >30 min. The idea of the external triggering of a substorm finds an answer also in a series of other studies (e.g., Lyons et al., 1997; Hsu and McPherron, 2004; Gallardo-Lacourt et al., 2012). At the same time, Wild et al. (2009) concluded that the existence of the southward IMF for not less than 22 min half an hour before T_o is a necessary condition for substorm onset and there is no need for an additional requirement of the northward turning of the IMF. Rare coincidences of northward-turning IMF with the onset of the substorm expansion phase can be treated as random phenomena related to the higher probability to the northward turning of the southward IMF. Newell and Liou (2011), supporting the viewpoint of Wild et al. (2009), concluded that substorms really need an initial elevation of solar wind activity; however, the presence of external triggering is not proved. Vorobjev et al. (2016) studied the state of the interplanetary medium in the periods of 112 isolated substorms. The results obtained in that study show that a northward-turning IMF is neither necessary nor sufficient for their generation.

Another problem discussed for many years is the region of explosive instability in the Earth's magnetosphere. There still exist two mutually exclusive viewpoints: some scientists believe that instabilities develop in the region of magnetic field line reconnection at distances of 15–20 R_E or even 20–25 R_E in the magnetosphere tail; others transfer this region to closed field lines in the capture region at distances of 5–7 R_E. A large number of published works support both points of view; for this reason, we dwell in more detail on our own experience and note that the most convincing arguments for the substorm onset inside the magnetosphere were presented for the first time by Lazutin (1979, 1986).

It is well known that a substorm begins with a sudden increase in auroral intensity at the equatorward edge of the oval, which is followed by expansion of the region of active auroras to the pole. The ion pressures at ionospheric heights and in the equatorial plane of the magnetosphere in magnetic quiet periods was compared (Antonova et al., 2014; Antonova et al., 2015; Kirpichev et al., 2016). It was shown that the equatorial boundary of the auroral oval in the midnight sector is projected to geocentric distances of 6–7 R_E. Localization of the equatorial boundary of the oval corresponds well to the dispersionless injection boundary position obtained by Lopez et al. (1990) and Spanswick et al. (2010).

Kirpichev et al. (2016) treated periods with $|AL| <$ 200 nT and $|Dst| < 10$ nT as magnetic quiet conditions. In the level of magnetic activity, these periods can include both quiet periods themselves and the substorm growth phase. Vorobjev et al. (2003) studied the position and dynamics of auroral precipitation boundaries in substorm periods. It was shown that the position of the oval equatorial boundary in the beginning of the substorm expansion phase approximately coincides with the position of the isotropization boundary (IB). In the magnetosphere, the isotropization boundary is predeterminedly positioned on closed geomagnetic field lines; in the period of substorm growth phase, when the field lines are stretched to the tail, the IB cannot move away but can only approach the Earth as compared to its position in quiet periods.

Thus, this work is based on a substorm model in which the magnetosphere is loaded–unloaded by the solar wind energy. The substorm begins at distances of 6–7 R_E in the form of a rapid development of an instability that does not require any external triggering for its onset.

The sources of energy for magnetospheric substorms are the solar wind plasma and interplanetary magnetic field. The results obtained in the scope of this investigation give reason to believe that quantitative characteristics of the solar wind plasma before the substorm growth phase create an equilibrium state in the Earth's magnetosphere that determines to a considerable extent the intensity of the magnetospheric

disturbance generated at a later stage. In other words, the dynamic pressure of the solar wind governs to a considerable extent the processes of magnetosphere loading–unloading and, therefore, determines the level of the magnetosphere–ionosphere disturbance.

Before the onset of the growth phase of an isolated substorm, the northward interplanetary magnetic field predominates. This thesis is illustrated by the behavior of the Bz IMF component in Figs. 1a and 1b. At $Bz \geq 0$; cross currents in the magnetosphere tail are insignificant, and the geomagnetic field has a dipole shape, both in the inner magnetosphere and at considerable distances from the Earth. In such periods, the magnetosphere is in the state of quasi-magnetostatic equilibrium is determined by the dynamic pressure of the solar wind P. With a change in P, the magnetosphere will change into a new equilibrium configuration. An increase of the level of the dynamics pressure of the solar wind will be accompanied by a corresponding increase in the plasma pressure in the plasma sheet (Tsyganenko and Mukai, 2003), which, in turn, will lead to a change in the magnitude and structure of the magnetosphere magnetic field, in particular, to the growth of B and an increase in its vertical component.

This can be indirectly indicated by the dynamics of negative values of the *Dst* index. Here, we are talking about the background state of the magnetosphere for 2–3 hours before the substorm. If the level of the velocity and dynamic pressure of the solar wind is low, $SYM/H \sim -(3–4)$ nT and next will be a weak substorm. If the level of V and P is high, $SYM/H \sim -(15–16)$ nT and next will be a considerable substorm (see Figs. 1 and 2). As can be seen, the SYM/H levels are low in the absolute value but differ from each other by four or five times.

With an increase of the pressure in the plasma sheet, the pressure inside the magnetosphere also increases. This will lead to an increase in the intensity of the DR current and, correspondingly, to a decrease in the SYM/H index. At the same time, an additional growth of the Bz component of the magnetic field will be observed in the outer part of the ring current.

The considerable level of the Bz component at distances of 6–10 R_E, on which the night sector of the aurora oval is projected under quiet geomagnetic conditions (Antonova et al., 2015; Kirpichev et al., 2016), is an obstacle for the development of instabilities leading to substorm generation. This seems to be evident for theories related to magnetic reconnection. However, in the theories based on the discontinuity of cross currents, the appearance of the magnetic field normal to the neutral layer creates difficulties in launching of the tearing instability (Lui et al., 1992).

In addition to this, the plasma sheet becomes denser and colder with an increase of the solar wind plasma density (and, correspondingly, dynamic pressure) at $Bz > 0$ (Terasava et al., 1997). This leads to a moderate increase in the fluxes of precipitating particles but to a decrease in the average energy for both precipitating electrons and ions. In general, the energy flux of precipitating electrons and intensity of the auroral 1NG N_2^+ 391.4 nm emission decrease with an increase of the plasma density (Vorobjev et al., 2004). As a consequence, the electron density and conductivity in the E layer of the ionosphere decrease, the intensity of ionospheric and field-aligned currents drops, and auroral arcs become weaker and/or disappear.

All the above factors create certain difficulties for substorm generation, regardless of whether the substorm is generated by an instability in the magnetosphere or triggered by the electrostatic instability developing in the region of outflowing field-aligned currents (Stepanova et al., 2002; Antonova et al., 2009).

The processes accompanying increasing dynamic pressure of the solar wind will result in the formation of conditions that increasingly impede substorm generation in the Earth's magnetosphere. Therefore, the higher the dynamic pressure is, the more solar wind energy must be pumped into the Earth's magnetosphere during the growth phase for substorm generation. At a later stage, this energy will be released during the substorm expansion phase and create even more intense magnetic bays.

6. CONCLUSIONS

The parameters of the IMF and solar wind plasma were investigated in the periods of registering 163 isolated magnetospheric substorms selected according to variations in the AL magnetic activity index. It was shown that the velocity V and plasma density N of the solar wind remain approximately constant for at least three hours before the onset of an isolated substorm T_o and one hour after T_o. Over the entire data array, the velocity of the solar wind on average demonstrates a stable trend to anticorrelation with its density. However, the situation is different if V and N are considered with respect to the intensity of substorms observed during that period. With an increase of the AL index in the substorm maximum, one can observe an increase in the levels both of velocity and density, on the background of which these substorms appear.

It was found that the value of the dynamic pressure P has a significant effect on the energy loading of the magnetosphere defined as the average values of functions E_{KL} and $d\Phi/dt$ during 1 h before the onset of each substorm. The increase of the dynamic pressure is accompanied by an increase in the loading energy necessary for substorm generation. Such interconnection between P and values of E_{KL} and $d\Phi/dt$ is absent in other arbitrarily chosen periods.

The results suggest that quantitative characteristics of the solar wind plasma before the substorm growth phase create an equilibrium state in the Earth's magnetosphere that determines to a considerable extent

the intensity of the magnetospheric disturbance generated at a later stage. Moreover, the processes accompanying the increasing dynamic pressure of the solar wind will result in the formation of conditions that increasing impede substorm generation in the Earth's magnetosphere. Therefore, the higher the dynamic pressure of the solar wind is, the more energy of it must be pumped into the Earth's magnetosphere during the growth phase for substorm generation. At a later stage, this energy will be released during the period of the substorm expansion phase and create all the more intense magnetic bays.

ACKNOWLEDGMENTS

This work was supported by the Presidium of the Russian Academy of Sciences, Program no. 28. The parameters of the IMF, solar wind plasma, and magnetic activity indices were taken from the web sites http://wdc.kugi.kyoto-u.ac.jp/ and http://cdaweb.gsfc.nasa.gov/.

REFERENCES

Antonova, E.E., Kornilov, I.A., Kornilova, T.A., Kornilov, O.I., and Stepanova, M.V., Features of auroral breakup obtained using data of ground-based television observations: case study, *Ann. Geophys.*, 2009, vol. 27, pp. 1413–1422. doi 10.5194/angeo-27-1413-2009

Antonova, E.E., Vorobjev, V.G., Kirpichev, I.P., and Yagodkina, O.I., Comparison of the plasma pressure distributions over the equatorial plane and at low altitudes under magnetically quiet conditions, *Geomagn. Aeron. (Engl. Transl.)*, 2014, vol. 54, no. 3, pp. 278–281. doi 10.7868/S001679401403002X

Antonova, E.E., Vorobjev, V.G., Kirpichev, I.P., Yagodkina, O.I., and Stepanova, M.V., Problems with mapping the auroral oval and magnetospheric substorms, *Earth Planets Space*, 2015, vol. 67, no. 1, id 166. doi 0.1186/s40623-015-0336-6

Barkhatov, N.A., Vorobjev, V.G., Revunov, S.E., and Yagodkina, O.I., Effect of solar dynamics parameters on the formation of substorm activity, *Geomagn. Aeron. (Engl. Transl.)*, 2017, vol. 57, no. 3, pp. 251–256. doi 10.1134/S0016793217030021

Boakes, P.D., Milan, S.E., Abel, G.A., Freeman, M.P., Chisham, G., and Hubert, B., A statistical study of the open magnetic flux content of the magnetosphere at the time of substorm onset, *Geophys. Res. Lett.*, 2009, vol. 36, L04105. doi 10.1029/2008GL037059

Gallardo-Lacourt, B., Nishimura, Y., Lyons, K.R., and Donovan, E., External triggering of substorms identified using modern optical versus geosynchronous particle data, *Ann. Geophys.*, 2012, vol. 30, pp. 667–673. doi 10.5194/angeo-30-667-2012

Hsu, T.-S. and McPherron, R.L., Average characteristics of triggered and nontriggered substorms, *J. Geophys. Res.*, 2004, vol. 109, A07208. doi 10.1029/2003JA009933

Kallio, E.I., Pulkkinen, T.I., Koskinen, H.E.J., et al., Loading–unloading processes in the nightside ionosphere, *Geophys. Res. Lett.*, 2000, vol. 27, no. 11, pp. 1627–1630. doi 10.1029/1999GL003694

Kan, J.R. and Lee, L.C., Energy coupling and the solar wind dynamo, *Geophys. Res. Lett.*, 1979, vol. 6, no. 7, pp. 577–580. doi 10.1029/GL006i007p00577

Kirpichev, I.P., Yagodkina, O.I., Vorobjev, V.G., and Antonova, E.E., Position of projections of the nightside auroral oval equatorward and poleward edges in the magnetosphere equatorial plane, *Geomagn. Aeron. (Engl. Transl.)*, 2016, vol. 56, no. 4, pp. 407–414. doi 10.7868/S0016794016040064

Lazutin, L.L., *Rentgenovskoe izluchenie avroral'nykh elektronov i dinamika magnitosfery* (X-Ray Emission of Auroral Electrons and Magnetospheric Dynamics), Leningrad: Nauka, 1979.

Lazutin, L.L., X-ray emissions of auroral electrons and magnetospheric dynamics, in *Physics and Chemistry in Space*, Berlin: Springer, 1986, vol. 14.

Li, H., Wang, C., and Peng, Z., Solar wind impact on growth phase duration and substorm intensity, *J. Geophys. Res.*, 2013, vol. 118, pp. 4270–4278. doi 10.1002/jgra.50399

Lopez, R.E., Sibeck, D.G., McEntire, R.W., and Krimigis, S.M., The energetic ion substorm injection boundary, *J. Geophys. Res.*, 1990, vol. 95, no. A1, pp. 109–117. doi 10.1029/JA095iA01p00109

Lui, A.T.Y., Lopez, R.E., Anderson, B.J., et al., Current disruptions in the near-Earth neutral sheet region, *J. Geophys. Res.*, 1992, vol. 97, no. A2, pp. 1461–1480. doi 10.1029/91JA02401

Lyons, L.R., Substorms: Fundamental observational features, distinction from other disturbances, and external triggering, *J. Geophys. Res.*, 1996, vol. 101, no. A6, pp. 13011–13026. doi 10.1029/95JA01987

Lyons, L.R., Blanchard, G.T., Samson, J.C., Lepping, R.P., Yamamoto, T., and Moretto, T., Coordinated observations demonstrating external substorm triggering, *J. Geophys. Res.*, 1997, vol. 102, no. A12, pp. 27039–27051. doi 10.1029/97JA02639

McPherron, R.L., Growth phase of magnetospheric substorms, *J. Geophys. Res.*, 1970, vol. 75, no. 28, pp. 5592–5599.

Milan, S.E., Grocott, A., Forsyth, C., Imber, S.M., Boakes, P.D., and Hubert, B., A superposed epoch analysis of auroral evolution during substorm growth, onset and recovery: Open magnetic flux control of substorm intensity, *Ann. Geophys.*, 2009, vol. 27, no. 2, pp. 659–668. doi 10.5194/angeo-27-659-20092

Newell, P.T. and Liou, K., Solar wind driving and substorm triggering, *J. Geophys. Res.*, 2011, vol. 116, A03229. doi 10.1029/2010JA016139

Newell, P.T., Sotirelis, T., Liou, K., Meng, C.-I., and Rich, F.J., A nearly universal solar wind–magnetosphere coupling function inferred from 10 magnetospheric state variables, *J. Geophys. Res.*, 2007, vol. 112, A01206. doi 10.1029/2006JA012015

Newell, P.T., Gjeroev, J.W., and Mitchell, E.J., Space climate implications from substorm frequency, *J. Geophys. Res.*, 2013, vol. 118, no. 10, pp. 6254–6265. doi 10.1002/jgra.50597

Newell, P.T., Liou, K., Gjeroev, J.W., Sotirelis, T., Wing, S., and Mitchell, E.J., Substorm probabilities are best predicted from solar wind speed, *J. Atmos. Sol.-Terr. Phys.*, 2016, vol. 146, pp. 28–37. doi 10.1016/j.jastp.2016.04.019

Russell, C.T. and McPherron, R.L., The magnetotail and substorms, *Space Sci. Rev.*, 1973a, vol. 15, nos. 2–3, pp. 205–266. doi 10.1007/BF00169321

Russell, C.T. and McPherron, R.L., Semiannual variation of geomagnetic activity, *J. Geophys. Res.*, 1973b, vol. 78, no. 1, pp. 92–108. doi 10.1029/JA78i001p00092

Shukhtina, M.A., Dmitrieva, N.P., Popova, N.G., Sergeev, V.A., Yahnin, A.G., and Despirak, I.V., Observational evidence of the loading–unloading substorm scheme, *Geophys. Res. Lett.*, 2005, vol. 32, L17107. doi 10.1029/2005GL023779

Shukhtina, M.A., Dmitrieva, N.P., and Sergeev, V.A., On the conditions preceding sudden magnetotail magnetic flux unloading, *Geophys. Res. Lett.*, 2014, vol. 41, no. 4, pp. 1093–1099. doi 10.1002/2014GL059290

Spanswick, E., Reeves, G.D., Donovan, E., and Friedel, R.H.W., Injection region propagation outside of geosynchronous orbit, *J. Geophys. Res.*, 2010, vol. 115. doi 10.1029/2009JA015066

Stepanova, M.V., Antonova, E.E., Bosqued, J.M., Kovrazhkin, R.A., and Aubel, K.R., Asymmetry of auroral electron precipitations and its relationship to the substorm expansion phase onset, *J. Geophys. Res.*, 2002, vol. 107, no. A7. doi 10.1029/2001JA003503

Terasawa, T., Fujimoto, M., Mukai, T., et al., Solar wind control of density and temperature in the near-Earth plasma sheet WIND/GEOTAIL collaboration, *Geophys. Res. Lett.*, 1997, vol. 24, no. 8, pp. 935–938. doi 10.1029/96GL04018

Tsyganenko, N.A. and Mukai, T., Tail plasma sheet models derived from Geotail particle data, *J. Geophys. Res.*, 2003, vol. 108, no. A3, 1136. doi 10.1029/2002JA009707

Vorobjev, V.G., Yagodkina, O.I., Starkov, G.V., and Feldstein, Y.I., A substorm in midnight auroral precipitation, *Ann. Geophys.*, 2003, vol. 21, no. 12, pp. 2271–2280. doi 10.5194/angeo-21-2271-2003

Vorobjev, V.G., Rezhenov, B.V., and Yagodkina, O.I., The solar wind plasma density control of night-time auroral particle precipitation, *Ann. Geophys.*, 2004, vol. 22, pp. 1047–1052. doi 10.5194/angeo-22-1047-2004

Vorobjev, V.G, Yagodkina O.I., and Zverev, V.L., Investigation of isolated substorms: Generation conditions and characteristics of different phases, *Geomagn. Aeron. (Engl. Transl.)*, 2016,vol. 56, no. 6, pp. 682–693. doi 10.7868/S001679400160601 6X

Wild, J.A., Woodfield, E.E., and Morley, S.K., On the triggering of auroral substorms by northward turnings of the interplanetary magnetic field, *Ann. Geophys.*, 2009, vol. 27, pp. 3559–3570. doi 10.5194/angeo-27-3559-2009

Translated by A. Nikol'skii